Raman Spectroscopic Study of Pressure Effects on the Spin-Crossover Coordination Polymers Fe(Pyrazine)[$M(CN)_4$]·$2H_2O$ (M = Ni, Pd, Pt). First Observation of a Piezo-Hysteresis Loop at Room Temperature

Gábor Molnár,[†,‡] Virginie Niel,[§] José-A. Real,[§] Leonid Dubrovinsky,[||] Azzedine Bousseksou,*[,†] and John J. McGarvey*[,‡]

Laboratoire de Chimie de Coordination, CNRS UPR-8241, 205 route de Narbonne, F-31077 Toulouse, France, School of Chemistry, The Queen's University of Belfast, Belfast BT9 5AG, Northern Ireland, U.K., Instituto de Ciencia Molecular, Universitat de Valencia, C/ Dr. Moliner 50, E-46100 Burjassot, Spain, and Bayerisches Geoinstitut, Universität Bayreuth, D-95440 Bayreuth, Germany

Received: November 25, 2002; In Final Form: February 7, 2003

The spin state of a series of cyanide-bridged iron(II) spin-crossover coordination polymers of formula Fe(pyrazine)[$M(CN)_4$]·$2H_2O$ (M = Ni, Pd, or Pt) have been studied by recording their solid-state Raman spectra at room temperature as a function of pressure. For the first time, a reproducible piezo-hysteresis loop has been observed at room temperature for the Ni complex with characteristic spin transition pressures of $P_{1/2}{}^{\uparrow} = 1350$ (±50) bar and $P_{1/2}{}^{\downarrow} = 650$ (±50) bar. For the Pd and Pt complexes, the spin-state change occurs around 1800 (±50) and 3500 (±500) bar, respectively, and competes with a pressure-induced structural transformation. Pressure effects on the spin state have been interpreted within the framework of an adapted two-level Ising-like model.

Introduction

The spin-crossover (SCO) phenomenon, involving thermo-, photo-, magneto-, and piezochromic properties of a class of transition metal complexes, is one of growing importance in the area of functional materials research, especially for applications in memory and display devices and as molecular switches.[1] The piezochromic properties of SCO materials have been recognized from the outset in spin-crossover research, with increasing pressure favoring the low-spin (LS) state because of its smaller volume and therefore shifting the spin equilibrium toward higher temperatures and accelerating the relaxation from the high-spin (HS) to the LS state at a given temperature. Indeed, many of the pioneering high-pressure spectroscopic studies of Drickamer[2] and Ferraro[3] in the 1970s addressed the SCO phenomenon using Mössbauer, UV−vis, and IR spectroscopies. High-pressure studies (using primarily Mössbauer detection) were taken up later by several groups.[4] On the whole, however, pressure effects remained less investigated than thermally and light-induced spin-state changes, mainly because of experimental difficulties.

There has been a renaissance of interest in the effect of pressure on SCO compounds during the 1990s, involving studies using either hydrostatic cells coupled to magnetic susceptibility,[5] optical absorption,[6] or reflectivity[7] detection methods or diamond anvil cells (DACs) in conjunction with IR,[8] EXAFS,[9] or X-ray diffraction[10] methods of detection. The latter group of techniques provide rich structural information, but the DAC technique is not well-adapted for the study of SCO materials in that pressure loops are difficult to record (especially at low temperatures), the most interesting pressure range (<10 kbar) is not easily accessible, and problems might arise from pressure gradients in the cells. Hydrostatic cells do not suffer from the above problems, and their large sample volumes might result in better signal-to-noise ratios. Using these various techniques, it has been possible to investigate the influence of pressure on the spin-transition temperature,[9] the thermal[5] and cryogenic piezo-hysteresis[7] cycles, the crystal structure,[10] and the relaxation process.[6,11]

The interpretation of pressure-induced changes (structural modifications, etc.) has sometimes been compromised by the relatively poor spectral information provided by the detection methods. For this reason, we have recently undertaken the development of a high-pressure Raman setup based on a hydrostatic high-pressure cell. We have chosen Raman spectroscopy because the spin-state change in these compounds can be conveniently followed by temperature- and pressure-dependent variations in their vibrational spectra.[1,12] Moreover, vibrational spectra contain information that can be employed to obtain structural[13] and bonding[1] information, as well as thermodynamic properties[12] of SCO complexes. Concerning the thermodynamic aspects, attention has been focused primarily on the entropy change associated with the SCO that stabilizes the HS form at high temperatures.[14] As pointed out by Sorai and Seki,[15] this entropy change is mostly vibrational in origin, although there are also contributions from the change in electronic configuration. The vibrational modes most affected by the change in spin state are the metal−ligand stretching and bending frequencies. Thus, the vibrational entropy change can be inferred, to a first approximation, from frequency shifts in the modes associated with the coordination sphere.[12]

In this paper, we report the first observation of a room-temperature (RT) piezo-hysteresis loop using our new high-pressure Raman setup. The systems chosen for study are a group of cyano-bridged coordination polymer compounds with the

* Corresponding authors. E-mail: j.mcgarvey@qub.ac.uk (J.J.M.), boussek@lcc-toulouse.fr (A.B.).
[†] CNRS UPR-8241.
[‡] The Queen's University of Belfast.
[§] Universitat de Valencia.
[||] Universität Bayreuth.

10.1021/jp027550z CCC: $25.00
Published on Web 03/14/2003

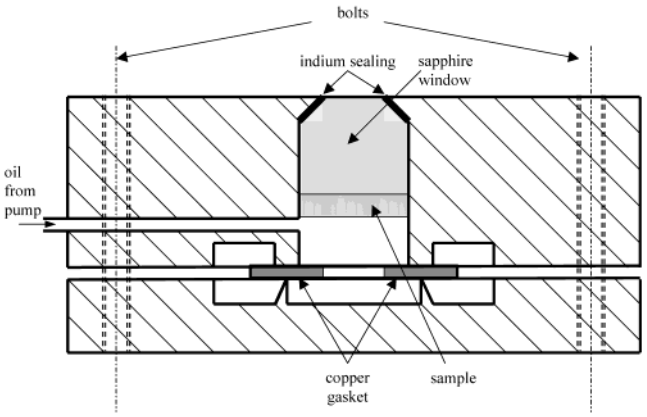

Figure 1. Schematic illustration of the high-pressure cell used for Raman measurements.

formula Fe(pyrazine)[$M(CN)_4$]·$2H_2O$ (M = Ni, Pd, or Pt, samples **I**, **II**, and **III**, respectively).[16] These compounds represent a qualitative and quantitative progress among polymeric SCO materials. The remarkable feature here is their unique 3D covalent polymeric structure giving rise to a highly cooperative spin transition associated with large thermal hysteresis loops. The spin transitions occur close to room temperature and are accompanied by pronounced color changes.

Experimental Section

Pure microcrystalline samples of **I**, **II**, and **III** were prepared according to ref 16.

A Spectra Physics 3900 Ti:sapphire laser pumped by an Ar^+ laser was used for Raman excitation at 785 nm. The laser power at the sample was ca. 100 mW, and the laser was focused to a line using a cylindrical lens. (Such a high laser power could be used because the pressure-transmitting medium effectively eliminates local heating effects.) Spectra were recorded by means of a CCD detector coupled to an HR640 Jobin-Yvon spectrograph (300 grooves/mm grating, 100-μm entrance slit) providing a spectral resolution of $\sim$3 cm^{-1}. Rayleigh scattering was removed using a holographic notch filter, and the Raman signals were collected at an angle of 180° to the incident laser beam in the 600−2300 cm^{-1} frequency range. Spectrograph calibration was carried out via a least-squares linear regression fit through a selection of solvent peaks (acetonitrile/toluene 50:50 mixture). Laser wavelength calibration was achieved using standard lines from a neon lamp.

For temperature runs at atmospheric pressure, the samples were placed into the copper sample holder of an Oxford Instruments Optistat-DN cryostat.

For pressure runs at RT, the samples were enclosed between two transparent polymer tapes in a high-pressure cell constructed for this experiment (Figure 1). This stainless steel cell (similar to that described in ref 7c) consists of two parts that are bolted together. A copper gasket is used to seal the cell. Optical access to the sample is provided by a 15-mm-thick sapphire window, which is sealed by an indium ring. The sample compartment is 7 mm deep and 10 mm in diameter, with a free aperture of 6 mm. Silicone oil (Edwards SF-702) was used as the pressure-transmitting medium. The oil enters the cell via a steel capillary soldered into the cell. Pressure is generated by means of a Nova-Swiss pump (550.03011) and is measured using an Intersonde pressure transducer (XT21). The accuracy of the pressure measurements was estimated to be ±50 bar using a calibrated Bourdon gauge. The pressure was increased in steps of 130 bar from atmospheric pressure to 2600 bar and then released in the same steps. Typical overshoot at high pressures was ca. ±20 bar, and the pressure was allowed to stabilize for 5 min before any measurements were made. Recording such a pressure cycle typically took 4−5 h, with acquisition times for individual Raman spectra of 1−3 min requiring a high-quality laser beam of constant energy.

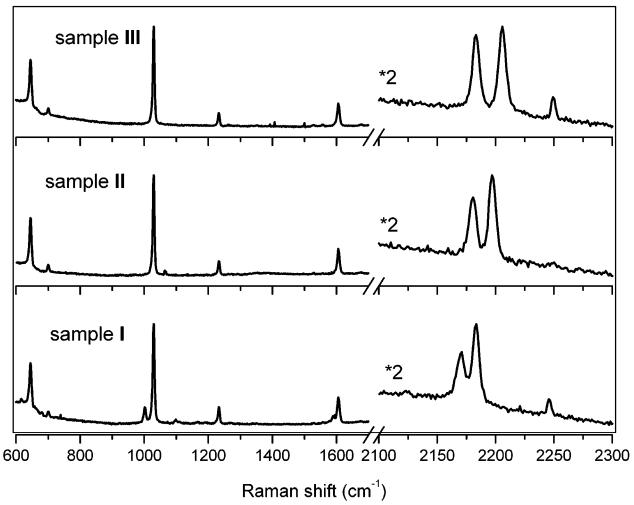

Figure 2. Raman spectra of samples **I**−**III** at room temperature and atmospheric pressure.

Samples **II** and **III** were also pressurized using a symmetric DAC with 600 mm flat culets.[17] The sample and ruby chips (3−5 mm in diameter) were loaded into a steel gasket hole ($\sim$300 μm in diameter, 250 μm thick, indented to a thickness of 150 μm) without any pressure-transmitting medium. Raman spectra of sample in the DAC were acquired in the 200−1200 cm^{-1} frequency range with acquisition times of 16 min using a micro-Raman system consisting of an Olympus BX40 microscope, a holographic notch filter, a single (1800 grooves/mm) grating spectrograph and a CCD detector. The entrance slit was kept at 120 μm, and a spectral resolution of ca. 2 cm^{-1} was obtained. In this configuration, the 632.8-nm line of a 30-mW He−Ne laser was used as the excitation source. The exciting radiation was directed through a neutral density filter (optical density of 0.6) and was focused on the sample via a ×50, long-working-distance objective. The scattered light was collected in a backscattering configuration using the same microscope objective. The spectrometer was regularly calibrated to the 520.7 cm^{-1} Si mode. Pressure in the DAC was determined by the ruby fluorescence method.[18] We also checked possible pressure gradients and found that, if any, the pressure differences were within the precision of the ruby scale (10−15%).

Results

In the frequency range investigated,[19] two main groups of Raman frequencies occur for each compound (Figure 2). Following our earlier assignments,[12b] these can be attributed to the CN stretching modes (around 2200 cm^{-1}) and to internal vibrations of pyrazine (between 1700 and 600 cm^{-1}). Even though both sapphire and silicone oil give rise to Raman signals in the high pressure cell, the CN modes, as well as certain pyrazine modes, are sufficiently well resolved to be employed as convenient spin-state marker bands. As an example, Figure 3 shows the evolution of the 675 cm^{-1} δ_{ring} pyrazine mode (an "LS marker band") as a function of temperature and pressure in sample **I**. We noted that, in addition to intensity changes, the different pyrazine modes also exhibited a slight (1−5 cm^{-1}) frequency shift under pressure, but we have not pursued this aspect further at present.

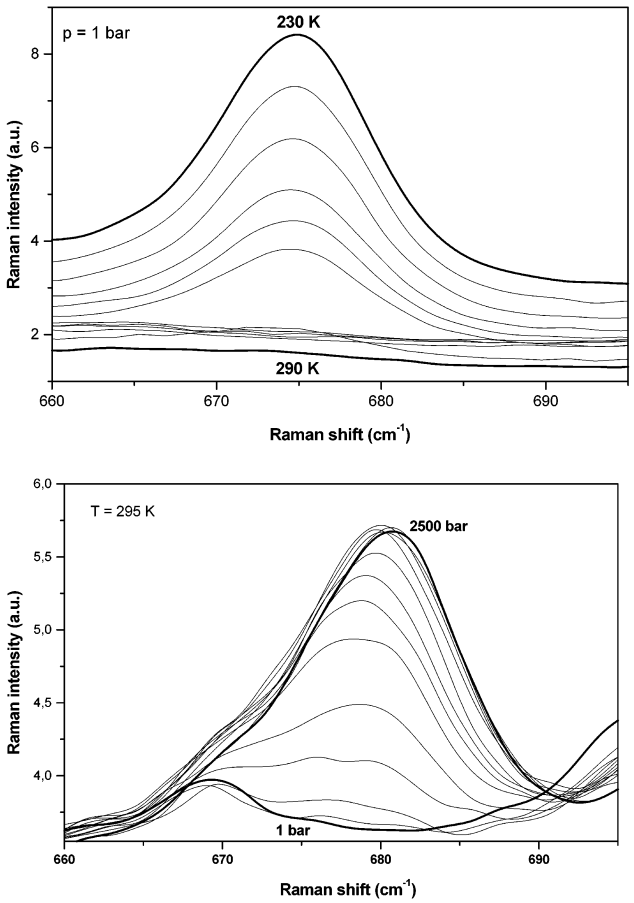

Figure 3. (a) Temperature dependence (from 230 to 290 K) of the 675 cm^{-1} Raman mode for sample **I**. (b) Pressure dependence (from 1 to 2500 bar) of the 675 cm^{-1} Raman mode for sample **I**.

We showed earlier that the two CN stretches are a sensitive probe for the identification of LS and HS forms in these compounds.[12b] As a general trend, in the HS state, these modes appear at lower frequencies (by ∼10 cm^{-1}) than in the LS phase. As shown in Figure 4a−c, the evolution of the ν_{CN} modes is more complex under pressure. For sample **III**, no well-defined LS band (2211, 2193 cm^{-1}) is observed up to 2600 bar, but three other CN modes appear around 2160, 2171, and 2194 cm^{-1} (Figure 4a). These modes grow in intensity between 100 and 900 bar, while the intensity of the HS modes (2204, 2182 cm^{-1}) decreases by about 60%. Then, between 900 and 2600 bar, no further change occurs. When the pressure is released, the original room-pressure HS spectrum is restored. In the case of sample **II**, similar changes occur between 500 and 1100 bar: the intensity of the HS modes (2181, 2197 cm^{-1}) decreases, and lower-frequency modes appear around 2174 and 2184 cm^{-1} (Figure 4b). As the pressure is increased further, between ca. 900 and 2400 bar, the LS modes (2192, 2205 cm^{-1}) appear, and their intensity increases at the expense of the HS modes. Again, releasing the pressure restores the original HS spectrum. In sample **I**, the CN modes are less intense and less well resolved. Their resolution is further complicated by the fact that there is an apparent HS residue in both the thermally-induced and the pressure-induced LS phase. However, as can be seen in Figure 4c, the CN bands are shifted to higher frequencies with pressure, indicating a HS-to-LS conversion. Definite evidence for the spin-state change in this compound was inferred from the appearance and growth of the 675 cm^{-1} pyrazine δ_{ring} mode with increasing pressure (Figure 3). This mode was observed previously only in the low-temperature LS phase and

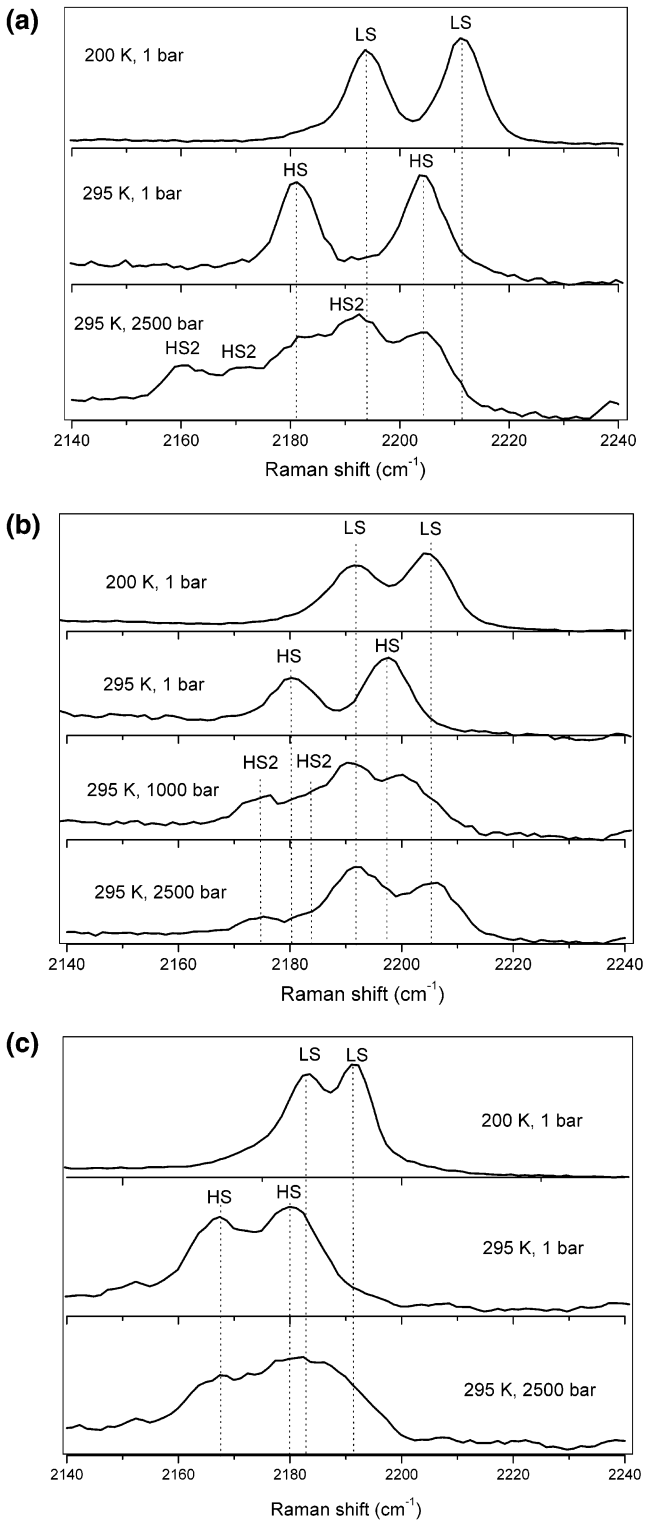

Figure 4. (a) Raman spectra (ν_{CN} modes) of samples (a) **III**, (b) **II**, and (c) **I** at different pressures and temperatures.

appears around 645 cm^{-1} in the HS phase.[12b] The pressure-induced spectral changes were found to be completely reversible and reproducible (through three successive pressure cycles) in this sample too.

In addition to frequency changes in the ν_{CN} spectral region, the pyrazine modes also display frequency shifts,[12b] and more importantly, their intensity increases considerably (by a factor of 10−100) upon the HS-to-LS transformation, allowing one to follow the spin transition quantitatively. The relationship between the Raman signal intensity and the HS fraction (γ_{HS})

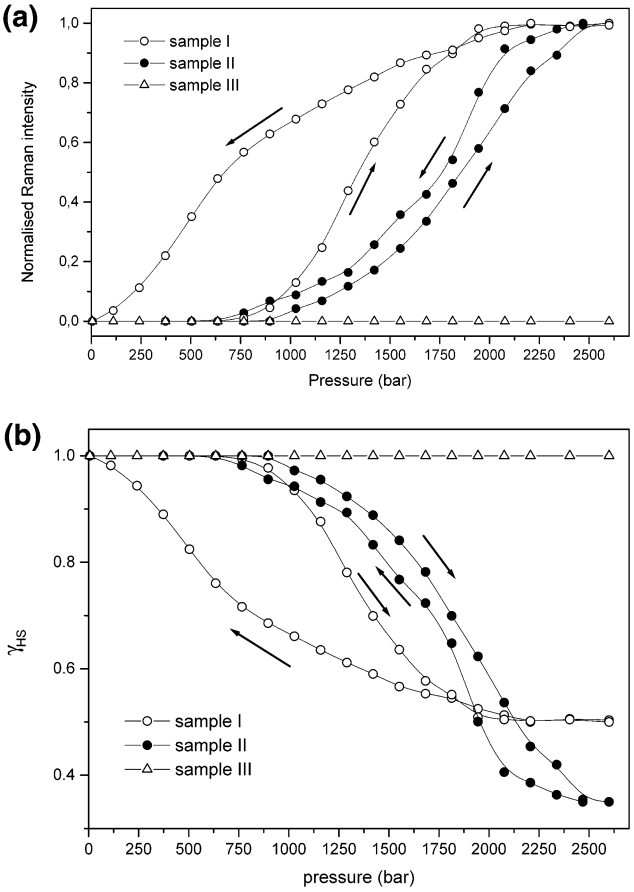

Figure 5. (a) Intensity of the 675 cm^{-1} LS marker band as a function of pressure for compounds **I**−**III** at room temperature. (Arrows indicate the increase and subsequent decrease of the pressure. Lines connecting the measurement points are included to guide the eye.) (b) HS fraction as a function of pressure evaluated from the Raman intensities taking into account the residual spin fractions. (Arrows indicate the increase and subsequent decrease of the pressure. Lines connecting the measurement points are included as a guide to the eye.)

is rather complex because of the accompanying color changes and surface effects. However, a comparison of the thermal spin-transition temperatures obtained from the Raman signal intensities and from magnetic susceptibility measurements showed that the former method gives a reasonable estimation for the variation of γ_{HS}.[12b] Figure 5a shows the intensity of the 675 cm^{-1} pyrazine δ_{ring} mode (LS marker band) as a function of pressure at room temperature, and Figure 5b represents γ_{HS} as a function of P obtained from the Raman intensities and corrected for the residual HS fractions. It should be noted that, by tracing the intensity of pyrazine modes around 1230 and 1605 cm^{-1}, we obtained transition curves that were identical, within experimental error, to those reported in Figure 5a.

As shown by Figure 5b, the spin transition in sample **II** is fairly gradual and centered around 1800 bar. The transition curves measured upon increasing and releasing the pressure are slightly different, but the experimental precision was not sufficient to confirm the existence of a piezo-hysteresis. On the other hand, sample **I** presents a large *pressure-hysteresis loop* with $P_{1/2}\uparrow$ of ∼1350 bar and $P_{1/2}\downarrow$ of ∼650 bar. For this sample, both pressure-induced and thermally[16] induced HS → LS transitions are incomplete, and the hysteresis loops are strongly deformed.

As discussed above, sample **III** shows no spin conversion up to 2600 bar. For this reason, we acquired Raman spectra of this sample at some higher pressures using the DAC technique

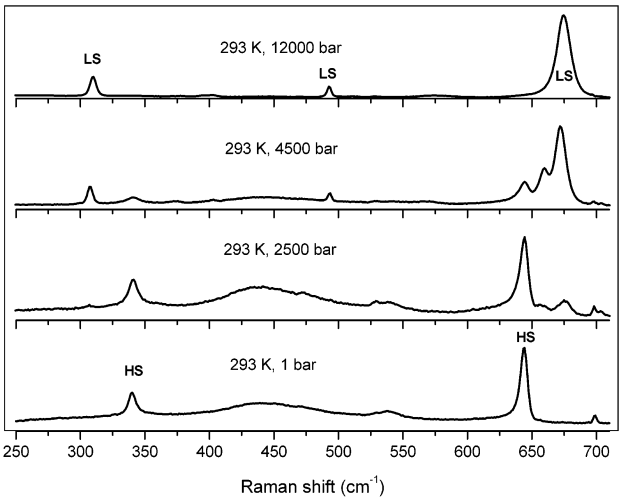

Figure 6. Raman spectra of sample **III** at different pressures using DAC for compression.

(Figure 6). According to our earlier study of temperature-dependent Raman spectra,[12b] the Raman modes around 311, 496, and 675 cm^{-1} are characteristic of the LS phase, whereas the modes around 341 and 644 cm^{-1} can be related to the HS form. As seen in Figure 6, upon pressurization, these latter modes disappear, while the former appear clearly, from which we can infer that, at higher pressures, this sample can also be switched to the LS state. Considering the transition pressure, the DAC technique that we used allows neither the fine adjustment of the pressure nor its precise determination; hence, we can establish only that $P_{1/2}$ for sample **III** has a value between 3000 and 4000 bar. We should also note the appearance and subsequent disappearance of a mode around 660 cm^{-1} that was not discernible in the temperature-dependent Raman spectra. This could be indicative of a structural distortion under pressure. Let us finally note that, when pressurized in the DAC, sample **II** exhibited LS Raman modes already at the onset of the pressurization (∼1−2 kbar) and the conversion to the LS state was quasi-complete at ∼3 kbar, in agreement with the (more detailed) observations made using the hydrostatic pressure cell.

Discussion

The first example of a pressure-induced hysteresis loop at cryogenic temperature (147 K) was reported recently by Codjovi et al.[7a] for the series of SCO compounds $Fe_{1-x}Ni_x(btr)_2(NCS)_2 \cdot H_2O$. These curves were subsequently analyzed using a Preisach-type model.[7b] It was found that pressure and temperature hysteresis loops could be transformed into each other, indicating a similar mechanism underlying the two phenomena. In the present paper a simple two-level Ising-like model adapted to pressure effects is proposed to analyze the experimental observations on compounds **I**−**III**, with particular reference to the origin of the pressure hysteresis loop.

Two-Level, Ising-like Model Including Pressure Effects. This model describes each metal center as a two level system. The intermolecular interactions are introduced through an Ising-like Hamiltonian. Following the formalism of ref 20, the two-level Hamiltonian, including cooperativity in the mean-field approach, is written as

$$\hat{H} = {}^1/_2\Delta\hat{\sigma} + J\hat{\sigma}\langle\hat{\sigma}\rangle \qquad (1)$$

where Δ is the energy gap ($\Delta = E_{HS} - E_{LS}$) of the isolated two-level system; $\hat{\sigma}$ is a fictitious spin operator, taking values

−1 (LS) and +1 (HS); and J is the interaction parameter. The spin fraction is derived as

$$n_{HS} = {}^1/_2\langle\hat{\sigma}\rangle + {}^1/_2 \quad (2)$$

that is, in this formalism, the spin conversion is characterized by the mean value of $\hat{\sigma}$. Considering $\langle\hat{\sigma}\rangle$ as a function of T, the following equation can be deduced[20]

$$\langle\hat{\sigma}\rangle = \frac{re^{-\beta(\Delta+2J\langle\hat{\sigma}\rangle)} - 1}{re^{-\beta(\Delta+2J\langle\hat{\sigma}\rangle)} + 1} \quad (3)$$

where $r = g_{HS}/g_{LS}$ with g_{HS} and g_{LS} being the degeneracies (of electronic and vibrational origins) associated with the two spin states.

The spin transition temperature, $T_{1/2}$ (defined as the temperature for which $\gamma_{HS} = {}^1/_2$), is obtained as

$$T_{1/2} = \Delta/\ln(r) \quad (4)$$

If one neglects any pressure dependence of J and g, the effect of pressure can be included in this model simply by replacing the energy term (Δ) in eqs 3 and 4 by

$$\Delta = \Delta^\circ + P\,\delta V \quad (5)$$

where Δ° is the energy gap at atmospheric pressure and δV is the volume change per molecule. $T_{1/2}$ now is expressed as

$$T_{1/2} = \Delta^\circ/\ln(r) + P\delta V/\ln(r) = T_{1/2}^\circ + P\delta V/\ln(r) \quad (6)$$

Using the formal relation $\Delta S = R\ln(r)$[14a] and taking into account that the $P\,\delta V$ term is expressed in Kelvin, one can deduce the macroscopic equivalent of eq 6 as

$$T_{1/2} = T_{1/2}^\circ + P\Delta V^p/\Delta S^p \quad (7)$$

where ΔV^p and ΔS^p are the (molar) variations in volume and entropy, respectively, associated with the pressure-induced spin-state conversion. Because we are interested in pressure hysteresis loops at fixed temperature (T_{fix}), eq 7 will be more useful in the form

$$P_{1/2} = (T_{fix} - T_{1/2}^\circ)(\Delta S^p/\Delta V^p) \quad (8)$$

where $P_{1/2}$ is defined as the pressure for which $\gamma_{HS} = {}^1/_2$.

It should be noted that the compressibility of the lattice and the pressure dependence of the vibrational frequencies in the two spin states are generally unknown. However, for relatively low pressures (i.e., a few kilobars), it is reasonable to assume that $\Delta S^p/\Delta V^p$ in eq 8 can be replaced by $\Delta S^\circ/\Delta V^\circ$. From different experiments on SCO complexes with an $Fe^{II}N_6$ core, this ratio was typically found to lie between 0.2 and 0.03 kbar/K.[4−9]

Discussion of the Model. The discontinuous character of *thermally induced* SCO (at atmospheric pressure) was first studied by Wajnflasz and Pick using an Ising-like model.[21] They noted that, if the interactions are strong, or more precisely if $J > T_{1/2}^\circ$, then the spin transition is discontinuous and can occur with hysteresis, whereas for the opposite case, the transition is gradual. The same conclusion was reached by Slichter and Drickamer, using a formally equivalent macroscopic model based on regular solution theory.[2]

The question that arises in the present instance centers on the conditions necessary to obtain a *pressure-induced* hysteresis cycle at a fixed temperature. Figure 7a shows the variation of

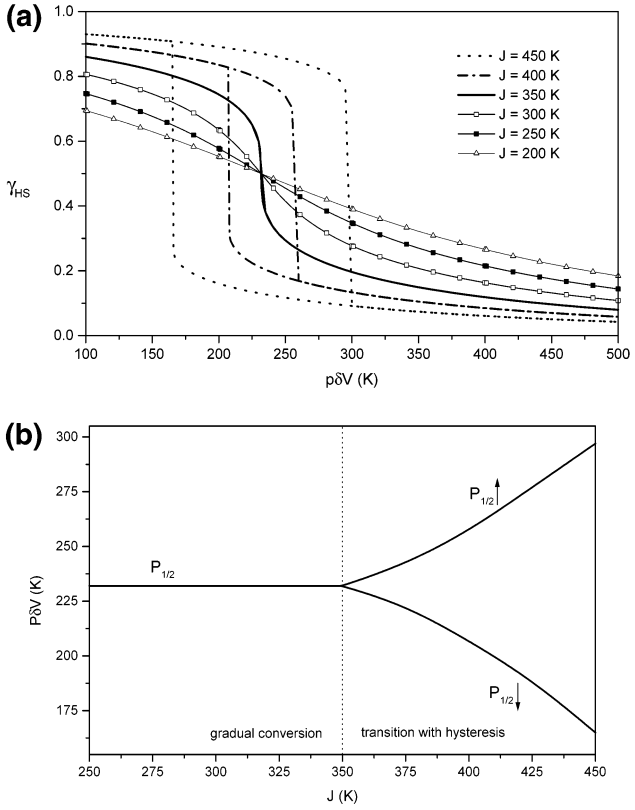

Figure 7. (a) Pressure-induced spin transition curves computed using eq 5 for different values of the intermolecular coupling J (with $g_{HS}/g_{LS} = 100$, $\Delta = 1380$ K, and $T = 350$ K). (b) Variation of $P_{1/2}$ as a function of J for the same parameter set as in Figure 7a.

γ_{HS} as a function of external pressure, computed using eqs 2, 3, and 5 for different values of the intermolecular coupling (J). As expected, the HS content decreases with increasing pressure. It is also confirmed that γ_{HS} varies discontinuously if $J > T_{fix}$; otherwise, it varies continuously and goes through ${}^1/_2$ at the same P value during increasing and decreasing pressure cycles (Figure 7b). It appears therefore that, if the intermolecular interactions are strong, not only is there a discontinuous jump in γ_{HS}, but a piezo-hysteresis loop also appears (provided that the system can remain at metastable minima). Taking into account eq 8, the condition to obtain a discontinuous pressure loop can also be written as $J > T_{1/2}^\circ + P_{1/2}\Delta V^p/\Delta S^p$. Because the second term is always positive, piezo-hysteresis can be expected *only* for complexes displaying thermal hysteresis at atmospheric pressure, which is the case for our samples.[16]

If $\Delta V^p/\Delta S^p$ is considered constant in the applied pressure range, the transition pressure ($P_{1/2}$) varies linearly with the measurement temperature (T_{fix}). Figure 8a,b illustrates this effect of the temperature on the pressure hysteresis. It is clearly seen that $P_{1/2}$ increases and also that the hysteresis width decreases with increasing temperature. The hysteresis disappears when $T_{fix} = J$. It should be remarked here that this condition affords an experimental means of determining the value of J, rather than using fitting procedures with the mean-field approximation, which are known to be inaccurate for reproducing hysteresis loops in highly cooperative systems.[20] To our knowledge, however, the piezo-hysteresis width has not yet been examined as a function of temperature (T_{fix}) for SCO complexes.

Considering the relation between $P_{1/2}$ and $T_{1/2}$, a linear dependence was found by Boillot et al.[9a] for several SCO compounds with $Fe^{II}N_6$ cores. Deviations from linearity were explained by assuming either molecular distortions or structural phase transitions under pressure. In our case, $T_{1/2}^\circ$ increases in

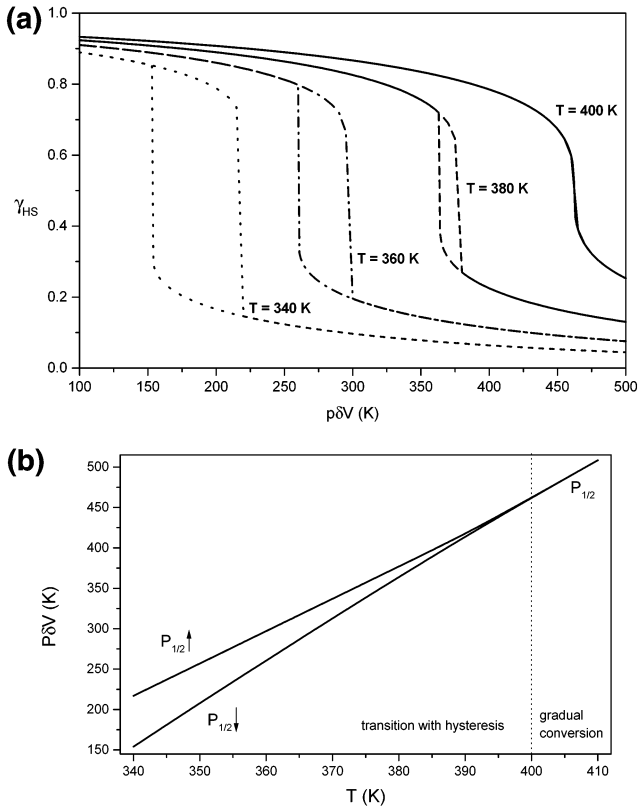

Figure 8. (a) Pressure-induced spin transition curves computed using eq 5, at different temperatures (with $g_{HS}/g_{LS} = 100$, $\Delta = 1380$ K, and $J = 400$ K). (b) Variation of $P_{1/2}$ as a function of T for the same parameter set as in Figure 8a.

the order **III** (250 K) < **II** (255 K) < **I** (265 K).[22] This might be one reason for the observed order of $P_{1/2}$, namely, **III** (~3500 bar) > **II** (1800 bar) > **I** (1000 bar), as well as for the absence of hysteresis in **II**. However, the differences in $T_{1/2}°$ are relatively small, and thus other factors that influence $P_{1/2}$ must also be considered. In fact, the observation of lower-frequency CN modes in samples **II** and **III** might be related to a pressure-induced structural transformation. This transformation must contribute to the shift of the spin transition to higher pressures in samples **II** and **III**. In other words, the formation of a new strucutural phase at the expense of the original HS phase competes with the formation of the LS phase under pressure. Concerning the nature of the new, pressure-induced phase, the number of Raman-allowed modes increases, from which a symmetry lowering can be inferred. One might speculate, for example, that the pressure distorts the quasi-planar arrangement of the Fe−NC−M bonds in the polymeric sheet leading to removal of the center of symmetry. In this new phase, the CN modes shift to lower frequencies, from which we can infer that the Fe(II) ions remain in the HS state. As a result, we can identify the new phase as a reduced-symmetry HS phase. Such a finding is not unprecedented: a similar mechanism has been suggested to explain the pressure-induced anomalous behavior of the polymeric SCO compound $Fe(btr)_2(NCS)_2 \cdot H_2O$.[5d,7a,9a]

Conclusions

We have reported here the first example of a reproducible piezo-hysteresis loop *at room temperature*, of relevance for potential applications of SCO materials.[1c] The fascinating feature here is the use of a perturbation other than temperature to obtain a memory effect. The theoretical analysis of pressure effects shows that hysteresis could occur during the pressure cycle if the interaction parameter exceeds the temperature of the experiment ($J > T_{fix}$). It appears also that a material exhibiting a thermal hysteresis loop is likely also to give rise a pressure loop, provided that this cycle is recorded at a temperature not much above $T_{1/2}°$. A more refined analysis of these phenomena is planned, taking into account short- and long-range interactions.

This investigation represents the first time that high-pressure Raman spectroscopy has been used to follow the pressure-induced spin-state change in SCO complexes. This method allowed us to record complete pressure cycles at fixed temperature and provided spectral evidence for the spin-state change and for other pressure-induced structural changes. Because the relationship between the Raman signal intensities and the HS fraction is not truly linear, the γ_{HS} vs P curves require calibration, for which high-pressure Mössbauer measurements are currently underway.

Acknowledgment. This work was supported by the European Community TMR Network TOSS (ERB-FMRX-CT98-0199). DAC experiments were performed at the Bayerisches Geoinstitut under the EU "IHP—Access to Research Infrastructures" program (HPRI-1999-CT-00004). G.M. acknowledges EC support through a Marie Curie Fellowship (HPMF-CT-2000-01026) and J.A.R. acknowledges the Ministerio Español de Ciencia y Tecnología (Project BQU-2001-2928). The authors are grateful to the LMOV (Versailles, France) for technical assistance. This article is dedicated to the memory of Dr. József Borossay.

References and Notes

(1) (a) Gütlich, P.; Hauser, A.; Spiering, H. *Angew. Chem., Int. Ed. Engl.* **1994**, *33*, 2024. (b) König, E. *Struct. Bonding (Berlin)* **1991**, *76*, 51. (c) Kahn, O. *Molecular Magnetism*; Wiley-VCH: New York, 1993.

(2) Slichter, C. P.; Drickamer, H. G. *J. Chem. Phys.* **1971**, *56*, 2142.

(3) Ferraro, J. R. *Coord. Chem. Rev.* **1979**, *29*, 1.

(4) (a) Meissner, E.; Köppen, H.; Kohler, C. P.; Spiering, H.; Gütlich, P. *Hyperfine Interact.* **1986**, *28*, 799. (b) Adler, P.; Spiering, H.; Gütlich, P. *J. Phys. Chem. Solids* **1989**, *50*, 587. (c) Pebler, J. *Inorg. Chem.* **1983**, *22*, 4125. (d) König, E.; Ritter, G.; Waigel, J.; Goodwin, H. A. *J. Chem. Phys.* **1985**, *83*, 3055. (e) Long, G. J.; Hutchinson, B. B. *Inorg. Chem.* **1987**, *26*, 608. (f) Köppen, H.; Meissner, E.; Wiehl, L.; Spiering, H.; Gütlich, P. *Hyperfine Interact.* **1989**, *52*, 29. (g) McCusker, J. K.; Zvagulis, M.; Drickamer, H. G.; Hendrickson, D. N. *Inorg. Chem.* **1989**, *28*, 1380.

(5) (a) Ksenofontov, V.; Levchenko, G.; Spiering, H.; Gütlich, P.; Létard, J. F.; Bouhedja, Y.; Kahn, O. *Chem. Phys. Lett.* **1998**, *294*, 545. (b) Ksenofontov, V.; Gaspar, A. B.; Real, J. A.; Gütlich, P. *J. Phys. Chem. B* **2001**, *105*, 12266. (c) Ksenofontov, V.; Spiering, H.; Schreiner, A.; Levchenko, G.; Goodwin, H. A.; Gütlich, P. *J. Phys. Chem. Solids* **1999**, *60*, 393. (d) Garcia, Y.; Ksenofontov, V.; Levchenko, G.; Schmitt, G.; Gütlich, P. *J. Phys. Chem. B* **2000**, *104*, 5045. (e) Niel, V.; Munoz, M. C.; Gaspar, A. B.; Galet, A.; Levchenko, G.; Real, J. A. *Chem. Eur. J.* **2002**, *8*, 2446. (f) Garcia, Y.; Ksenofontov, V.; Levchenko, G.; Gütlich, P. *J. Mater. Chem.* **2000**, *10*, 2274.

(6) (a) Schenker, S.; Hauser, A.; Wang, W.; Chan, I. Y. *Chem. Phys. Lett.* **1998**, *297*, 281. (b) Hauser, A.; Romstedt H.; Jeftic, J. *J. Phys. Chem. Solids* **1996**, *57*, 1743. (c) Jeftic, J.; Kindler, U.; Spiering, H.; Hauser, A. *Meas. Sci. Technol.* **1997**, *8*, 479. (d) Jeftic, J.; Hauser, A. *Chem. Phys. Lett.* **1996**, *248*, 458. (e) Jeftic, J.; Hinek, R.; Capelli, S. C.; Hauser, A. *Inorg. Chem.* **1997**, *36*, 3080. (f) Jeftic, J.; Hauser, A. *J. Phys. Chem. B* **1997**, *101*, 10262.

(7) (a) Codjovi, E.; Menéndez, N.; Jeftic, J.; Varret, F. *C. R. Acad. Sci. IIC* **2001**, *4*, 181. (b) Enachescu, C.; Constant-Machado, H.; Menendez, N.; Codjovi, E.; Linares, J.; Varret, F.; Stancu, A. *Physica B* **2001**, *306*, 155. (c) Jeftic, J.; Menendez, N.; Wack, A.; Codjovi, E.; Linares, J.; Goujon, A.; Hamel, G.; Klotz, S.; Syfosse, G.; Varret, F. *Meas. Sci. Technol.* **1999**, *10*, 1059.

(8) Sunatsuki, Y.; Sakata, M.; Matsuzaki, S.; Matsumoto, N.; Kojima, M. *Chem. Lett.* **2001**, *12*, 1254.

(9) (a) Boillot, M. L.; Zarembowitch, J.; Itié, J. P.; Polian, A.; Bourdet, E.; Haasnot, J. P. *New J. Chem.* **2002**, *26*, 313. (b) Roux, C.; Zarembowitch, J.; Itié, J. P.; Polian, A.; Verdaguer, M. *Inorg. Chem.* **1996**, *35*, 574. (c) Roux, C.; Zarembowitch, J.; Itié, J. P.; Verdaguer, M.; Dartyge, E.; Fontaine, A.; Tolentino, H. *Inorg. Chem.* **1991**, *30*, 3174. (d) Hannay, C.; Hubin-

Franskin, M. J.; Grandjean, F.; Briois, V.; Itié, J. P.; Polian, A.; Trofimenko, S.; Long, G. J. *Inorg. Chem.* **1997**, *36*, 5580.

(10) (a) Guionneau, P.; Brigouleix, C.; Barrans, Y.; Goeta, A. E.; Létard, J. F.; Howard, J.; Gaultier, J.; Chasseau, D. *C. R. Acad. Sci. IIC* **2001**, *4*, 161. (b) Granier, T.; Gallois, B.; Gaultier, J.; Real, J. A.; Zarembowitch, J. *Inorg. Chem.* **1993**, *32*, 5305.

(11) (a) McGarvey, J. J.; Lawthers, I.; Heremans, K.; Toftlund, H. *Inorg. Chem.* **1990**, *29*, 252. (b) McGarvey, J. J.; Lawthers, I.; Heremans, K.; Toftlund, H. *J. Chem. Soc., Chem. Commun.* **1984**, 1575. (c) DiBenedetto, J.; Arkle, V.; Goodwin, H. A.; Ford, P. C. *Inorg. Chem.* **1985**, *24*, 455.

(12) (a) Bousseksou, A.; McGarvey, J. J.; Varret, F.; Real, J. A.; Tuchagues, J. P.; Dennis, A. C.; Boillot, M. L. *Chem. Phys. Lett.* **2000**, *318*, 409. (b) Molnár, G.; Niel, V.; Gaspar, A. B.; Real, J. A.; Zwick, A.; Bousseksou, A.; McGarvey, J. J. *J. Phys. Chem. B* **2002**, *106*, 9701. (c) Moliner, N.; Salmon, L.; Capes, L.; Carmen-Munoz, M.; Létard, J. F.; Bousseksou, A.; Tuchagues, J. P.; McGarvey, J. J.; Dennis, A. C.; Castro, M.; Burriel, R.; Real, J. A. *J. Phys. Chem. B* **2002**, *106*, 4276.

(13) Tayagaki, T.; Tanaka, K. *Phys. Rev. Lett.* **2001**, *86*, 1351.

(14) (a) Bousseksou, A.; Constant-Machado, H.; Varret, F. *J. Phys. I Fr.* **1995**, *5*, 747. (b) Sorai, M. *Bull. Chem. Soc. Jpn.* **2001**, *74*, 2223.

(15) Sorai, M.; Seki, S. *J. Phys. Chem. Solids* **1974**, *35*, 555.

(16) Niel, V.; Martinez-Agudo, J. M.; Munoz, M. C.; Gaspar, A. B.; Real, J. A. *Inorg. Chem.* **2001**, *40*, 3838.

(17) The grain size of sample **I** was incompatible with the DAC volume, and grinding could not be applied because it removes the SCO property of the sample.

(18) Mao, H. K.; Xu, J.; Bell, P. M. *J. Geophys. Res.* **1986**, *91*, 4673.

(19) Raman modes below 600 cm^{-1} could not be used for intensity reasons.

(20) Bousseksou, A.; Nasser, J.; Linares, J.; Boukheddaden, K.; Varret, F. *J. Phys. I Fr.* **1992**, *2*, 1381.

(21) Wajnflasz, J.; Pick, R. *J. Phys. IV Fr.* **1971**, *32*, C1.

(22) $T_{1/2}°$ values were determined by magnetic susceptibility measurements on the same preparation that was investigated under pressure. It should be noted that these values are somewhat different from those reported in ref 16, as a result of small deviations from batch to batch.